Virology 535 (2019) 200–209

Contents lists available at ScienceDirect

Virology

journal homepage: www.elsevier.com/locate/virology

Host factor heat-shock protein 90 contributes to baculovirus budded virus morphogenesis via facilitating nuclear actin polymerization

Shufen Li, Yun Wang, Dianhai Hou, Zhenqiong Guan, Shu Shen, Ke Peng, Fei Deng, Xinwen Chen, Zhihong Hu, Hualin Wang, Manli Wang*

State Key Laboratory of Virology, Wuhan Institute of Virology, Chinese Academy of Sciences, Wuhan, 430071, China

ARTICLE INFO

Keywords:
Hsp90
Baculovirus
BV morphogenesis
F-actin
Regulatory mechanism

ABSTRACT

Hsp90, a highly conserved cellular molecular chaperone, is involved in the life cycle of many viruses. A recent proteomics study revealed that Hsp90 was incorporated into the budded virions (BVs) of baculovirus, we therefore explored the role of Hsp90 during Autographa californica multiple nucleopolyhedrovirus (AcMNPV) infection process. The results showed that Hsp90 was essential for AcMNPV BV propagation in cultured cells. Electron microscopy detected that nucleocapsids failed to egress from the nucleus to the cytoplasm for further BV budding. Inactivation of Hsp90 abolished virus-triggered nuclear actin polymerization, a process providing essential driving forces for nucleocapsid egress. Further analyses suggested that this was due to the selectively regulation of the proper protein levels and nuclear accumulation of P40 subunit of host actin related protein 2/3 complex (Arp2/3). Thus, Hsp90 participates in baculovirus BV propagation by facilitating nuclear actin polymerization required for progeny BV production.

1. Introduction

Baculoviruses comprise a diverse group of large DNA viruses, which have important applications in the areas of insect pesticides, protein expression and gene therapy, *etc.* (Ghosh et al., 2002; Inceoglu et al., 2001; Kidd and Emery, 1993). Two morphologically distinct and temporally regulated progeny phenotypes are produced in a biphasic life cycle: the budded virus (BV) and the occlusion-derived virus (ODV) (Keddie et al., 1989). ODV infects the epithelial cells of insect midgut to initiate primary infection, while BV is transmitted from cell to cell and cause systemic infection (Summers, 1971; Volkman and Summers, 1977).

Successful virus infection involves in complicated and dedicated virus-host interactions. In comparison to medically important human viruses such as human immunodeficiency virus (HIV) and herpesvirus (HSV) (de Chassey et al., 2008; Jager et al., 2012; Uetz et al., 2006), the area of virus-host interaction of baculoviruses is relatively obscure. Actin may represent one of the best studied host factors involved in baculovirus life cycle. Both retrograde and anterograde cytoplasmic transports of nucleocapsid are dependent on actin cytoskeleton. In addition, baculovirus infection will lead to the translocation of monomeric actin (G-actin) from cytoplasm into nucleus and the subsequent polymerization of G-actin within nucleus, which requires co-action of both viral proteins and a set of host factors (Charlton and Volkman, 1993; Kasman and Volkman, 2000; Lanier and Volkman, 1998). Among them, viral protein P78/83 functions as a nucleation promoting factor (NPF) to interact with host actin related protein 2/3 complex (Arp2/3) for actin polymerization, and this process is controlled by a regulatory cascade involving BV/ODV-C42 and Ac102 (Wang et al., 2008b; Zhang et al., 2018). The nuclear filamentous actin (F-actin) was known to be required for AcMNPV morphogenesis (Lanier and Volkman, 1998; Ohkawa and Volkman, 1999) and a recent study revealed its crucial role in the egress of progeny viral nucleocapsids from the nucleus to the cytoplasm for BV formation (Ohkawa and Welch, 2018). Apart from actin, accumulating transcriptomic- and proteomic analyses have revealed possible interactions between baculoviruses and hosts (Chen et al., 2013; Hou et al., 2013; Wang et al., 2010c). Among those, an important molecular chaperone heat-shock protein 90 (Hsp90) raised our interest.

Hsp90 is an abundant and highly conserved molecular chaperone that belongs to the Hsp family in both prokaryotes and eukaryotes (Pearl and Prodromou, 2006). Hsp90 possesses important functions in the conformational maturation and transportation of a variety of proteins and protein complex, including transcription factors, steroid receptors, and protein kinases, which are involved in signal transduction and cell cycle control (Picard, 2002; Pratt and Toft, 2003). Hsp90 was

* Corresponding author.
E-mail address: wangml@wh.iov.cn (M. Wang).

https://doi.org/10.1016/j.virol.2019.07.006
Received 25 February 2019; Received in revised form 3 July 2019; Accepted 4 July 2019
Available online 05 July 2019

identified as a promising novel target for anti-tumor therapy (Li et al., 2009). In the cycle of Hsp90-assisted protein maturation, nascent polypeptide firstly interacts with Hsp40/Hsp70 chaperones then transferred to Hsp90 by Hsp70 and Hsp90 organizing protein (HOP). After binding of ATP to the N-terminal domain of Hsp90 complex, HOP and Hsp70 are replaced by other co-chaperones. The bound ATP is hydrolyzed by the N-terminal ATPase activity of Hsp90, resulting in the folding and release of the client proteins (Jackson, 2013; Wandinger et al., 2008). The N-terminal ATPase activity of Hsp90 is critical for its chaperon function. Specific Hsp90 inhibitors, such as Geldanamycin (GA) and its derivatives are known to inhibit the function of Hsp90 by competitive binding to the unique ADP/ATP binding site (McClellan and Frydman, 2001), resulting in unsuccessful folding and the subsequent proteasomal degradation of the client proteins (Jackson, 2013).

GA and its derivatives have been widely used to investigate the biological functions of Hsp90. By using these inhibitors, the involvement of Hsp90 in the life cycles of many viruses has been recognized. For example, inhibition of Hsp90 had a profound effect on the entry of enterovirus 71 (EV71), replication of Ebola virus and assembly or trafficking of nucleocapsids of hepatitis E virus and respiratory syncytial virus (Das et al., 2014; Radhakrishnan et al., 2010; Smith et al., 2010; Tsou et al., 2013; Zheng et al., 2010). In addition, Hsp90 was identified as a component of receptor complex in the entry of dengue virus and infectious bursal disease virus (IBDV) (Lin et al., 2007; Reyes-Del Valle et al., 2005). Several viral proteins, such as the RNA polymerase subunits of influenza virus, the DNA polymerase of HSV-1, the large T antigen of simian virus 40, the reverse transcriptase of hepatitis B virus and the NS2/3 of hepatitis C virus, have been defined as client proteins of Hsp90 (Burch and Weller, 2005; Hu and Seeger, 1996; Miyata and Yahara, 2000; Naito et al., 2007; Ujino et al., 2009; Waxman et al., 2001). These data suggested different but significant roles of Hsp90 in the life cycles of many viruses.

17-AAG, a derivative of GA, was reported to decrease the DNA synthesis of Autographa californica multiple nucleopolyhedrovirus (AcMNPV) in cultured cells (Lyupina et al., 2011). This evidence, along with the proteomics data, suggests the involvement of Hsp90 in baculovirus infection. In this study, we comprehensively depicted the role of Hsp90 in the life cycle of AcMNPV. By using the Hsp90 specific inhibitor GA and RNAi strategy, Hsp90 was found to be essential for AcMNPV propagation, particularly in BV morphogenesis. The possible mechanism was further investigated, and we showed that Hsp90 regulates baculovirus progeny BV production through participating in the protein levels and nuclear accumulation of host Arp2/3-P40 subunit, which is required for the nuclear polymerization of actin.

2. Material and methods

2.1. Cells and viruses

Spodoptera frugiperda Sf9 cells (Vaughn et al., 1977) were maintained in Grace's insect medium (pH 6.0; Gibco-BRL), supplemented with 10% fetal bovine serum (FBS; Gibco-BRL) at 27 °C. Wild type (WT) AcMNPV E2 strain was stocked in our laboratory. vAc-*egfp*, a recombinant AcMNPV with an enhanced green fluorescent protein (*egfp*) reporter gene was constructed previously (Dong et al., 2010). vAc-*rfp*, a recombinant AcMNPV with a red fluorescent protein (*rfp*) reporter gene driven by the Orgyia pseudotsugata multinucleocapsid nuclear polyhedrosis virus (OpMNPV) *gp64* promoter (Op166) was generated by transposition of transfer vector pFB-Op166-*rfp* (Wang et al., 2010b) into AcBacmid to generate recombinant bacmid Ac-*rfp*, followed by transfection of the bacmid DNA into Sf9 cells to produce the recombinant virus (Bac-to-Bac manual, Invitrogen).

2.2. Gene cloning and antibody generation

The entire ORF of *S. frugiperda hsp90* gene was amplified with primer pair Hsp90-For: 5′-ATGCCCGAAGAAATGCAGAC-3′ and Hsp90-Rev: 5′-TTAATCCACTTCCTCCATACG-3′, using genomic DNA of Sf9 cells as template (Landais et al., 2001). The PCR product was cloned into pGEM-T Easy vector (Promega). The construct was sequenced and aligned with the sequence download from NCBI (GenBank accession number: AF254880.1), the alignment result indicated that correct hsp90 gene was cloned (with only 1 nt different). For the generation of antibody against Hsp90, the *hsp90* gene was digested from pGEM-T Easy vector by *Eco*RI and inserted into pET28a expression vector site. Proteins were purified and used to immune rabbit to generate specific *anti*-hsp90 polyclonal antibody (Zou et al., 2016).

2.3. Detection of Hsp90 localization in BVs and ODVs

AcMNPV BVs and ODVs were propagated and purified as described previously (Wang et al., 2010c). Purified BV and ODV preparations were separated into envelope and nucleocapsid fractions as described before (Wang et al., 2018) and subjected to Western blot analysis with primary antibodies as follows: *anti*-Hsp90, *anti*-ODV-E66, *anti*-GP64 and *anti*-VP39.

2.4. Plaque assay

Sf9 cells were infected with vAc-*egfp* at an MOI of 0.01 and allowed to adsorb for 1 h at 4 °C. The supernatant was removed, and cells were treated with 1.25 μM GA (purchased from Sigma-Aldrich, stocked in DMSO and diluted in Grace's medium) or with equal concentration of DMSO as the control, and incubated at 27 °C. At 18 h post infection (h p.i.), cells were covered with low melting temperature agarose and plaque formation was observed under a fluorescence microscope at 48 h p.i.

2.5. Quantitative PCR analyses of AcMNPV replication and BV production

Sf9 cells (5×10^5 per well; 24-well plates) were infected with vAc-*egfp* at an MOI of 5 and incubated at 27 °C for 1 h. The supernatant was removed and the cells were treated with different concentration of GA (0.156, 0.313, 0.625 and 1.250 μM) or DMSO control. At 24 h p.i., the infected cells and the supernatant was harvested, respectively. The infection experiment was done in triplicate. For AcMNPV replication analysis, the infected cells were washed with PBS three times and subjected to genomic DNA isolation using Axyprep Multisource Genomic DNA Miniprep kit (Axygen). Total cellular DNA isolated from each well was dissolved in 50 μl ddH_2O and 5 μl aliquot was used as template and subjected to quantitative PCR (qPCR) analysis to determine viral DNA copy numbers in infected cells, using primers *vp80*-For: 5′-GACGATGTCGTTAATCGTGC-3′ and *vp80*-Rev: 5′-ATCAGCATC GCTATTCAGATAA-3’. The qPCR was carried out as described previously (Wang et al., 2008a). For BV production analysis, 100 μl of supernatant from each well was used to isolate viral DNA (Wang et al., 2010a). Total viral DNA was dissolved in 50 μl ddH_2O and 5 μl were used as template for qPCR analysis as described above.

To assess the impact of Hsp90 inhibition on viral DNA replication, Sf9 cells (1×10^6 per well; 35-mm-diameter well) were transfected with 1 μg AcΔ*gp64* bacmid (Wang et al., 2008a) and treated with GA (1.25 μM) or DMSO control. At 24 and 48 h post transfection (h p.t.), total cellular DNA was isolated and dissolved in 40 μl ddH_2O. After incubation with DpnI (New England BioLabs) to remove residual bacmid DNA, 1 μl of the digested DNA was used for qPCR analysis as described above.

2.6. RNAi assay

To produce double-stranded RNA, approximately 340-bp DNA fragment from the *Sf-hsp90* gene was amplified by using PCR with the sense primer: 5′-TAATACGACTCACTATAGGGTCGACAGTGAGGACC

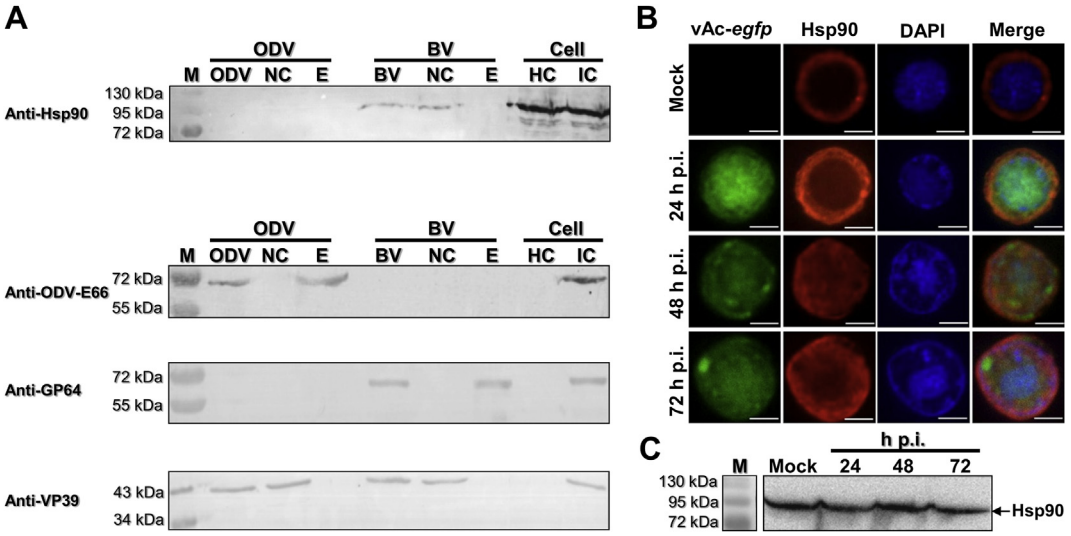

Fig. 1. Localization and expression of Hsp90. (A) Localization of Hsp90 in AcMNPV virions. BV and ODV were purified, fractionated into nucleocapsid and envelope component and proteins were detected by Western blot analyses. Hsp90 and the internal controls, including ODV envelope protein E66, BV envelope protein GP64 and the major nucleocapsid protein VP39 were detected with their respective antibodies. NC, nucleocapsid fraction; E, envelope fraction; HC, healthy cells; IC, infected cells. (B) The subcellular distribution of Hsp90 in healthy cells and in AcMNPV infected cells by imunofluorescence assay. Sf9 cells were infected with vAc-*egfp* (MOI = 5). The localization of Hsp90 in infected cells was analyzed by IF microscopy using *anti*-Hsp90 antibody. Nuclei were stained with DAPI. Fluorescence was visualized by confocal microscopy at 24, 48, 72 h p.i.. Bars represent 5 μm. (C) Expression levels of Hsp90 in healthy cells or AcMNPV infected cells. Sf9 cells were mock-infected or infected with vAc-*egfp* at an MOI of 5. At 24, 48 and 72 h p.i., cells were harvested for Western blot analysis by using *anti*-Hsp90 antibody.

TGC-3′ and the antisense primer: 5′- TAATACGACTCACTATAGGGACC TGGTCACGGTTCTCA.

C-3' (T7 RNA polymerase binding site underlined). The PCR product was purified by using a DNA isolation system (OMEGA) and dsRNA was generated and purified by *in vitro* transcription using a MEGAscript RNAi kit (Thermo fisher).

For RNAi assay, Sf9 cells (5×10^5 per well) in 24-well tissue culture plate were transfected with 12 μg dsRNA against *hsp90* or non-specific dsRNA targeting eGFP by using lipofectin (Invitrogen). At 24 h p.t., cells were infected with vAc-*egfp* (MOI = 5). At 24 h p.i., 100 μl of each supernatant was harvested to isolate BVs and measured genomic DNA copy numbers as described above. Cells were collected to detect the inhibition efficiency by Western blot. The experiment was repeated twice.

2.7. Electron microscopy (EM) of infected cells

Sf9 cells (2×10^6) were incubated with vAc-*egfp* (without a *polyhedrin* gene) or AcMNPV at an MOI of 5 and incubated at 27 °C for 1 h. The supernatant was removed and the cells were treated with either GA (1.25 μM), cytochalasin D (CD, 2 μg/ml) or DMSO as control. To observe BV budding, cells were harvested at 24 and 36 h p.i.. For EM sample preparation, cells were washed three times with PBS, fixed with 2.5% (W/V) glutaraldehyde in 0.1 M sodium chlorideand processed for EM as previously described (Li et al., 2018). BV morphogenesis was observed under a transmission electron microscope (FEI Tecnai G2 microscope at 200 kV).

2.8. Western blot analysis of the abundance of viral- and host proteins

To examine the effect of Hsp90 inhibition on viral P78/83 protein abundance, Sf9 cells (2×10^6) were incubated with vAc-*egfp* at an MOI of 5 at 27 °C for 1 h. The supernatant was removed, and the cells were treated with GA at a concentration of 1.25 μM or DMSO as control. At 48 h p.i., infected cells were disrupted in 4 × SDS-PAGE sample buffer, and proteins were separated on 12% SDS-PAGE and further transferred onto PVDF membranes (Millipore) by semi-dry electrophoresis. Western blot analyses were performed with rabbit antisera against P78/83 (Wang et al., 2008b) and Hsp90 as the primary antibody, and alkaline phosphatase (AP)-conjugated goat anti-rabbit immunoglobulin (Jackson ImmunoResearch) as the secondary antibody. The final signals were detected with NBT/BCIP (Amresco).

To examine the effect of Hsp90 inhibition on the accumulation of actin and P40 subunit of Arp2/3 complex in presence or absence of GA treatment. Sf9 cells were transfected with plasmid pIZ/V5-*actin-egfp* (Sf9 *actin* fused with *egfp*) or pIZ/V5-*p40*-HA (Han et al., 2012). To analyze the accumulation of P40 and actin in Sf9 cells, transfected cells were super-infected with vAc-*rfp* (MOI = 5) at 24 h p.t., treated with either GA or DMSO and collected at 24, 36 and 48 h post drug treatment. All the samples were analyzed by Western blots using *anti*-EGFP polyclonal antibody or anti-HA monoclonal antibody (Beyotime, P.R. China) as the primary antibody and the AP-conjugated goat anti-rabbit immunoglobulin or AP-conjugated goat anti-mouse IgG (Proteintech) as the secondary antibody.

2.9. Fluorescence and immunofluorescence (IF) microscopy

The subcellular localization of Hsp90 was observed by imunofluorescence assay, Sf9 cells (2×10^6) were infected with vAc-*egfp* at an MOI of 5. At 24, 48 and 72 h p.i., the cells were fixed and permeabilized. The cells were blocked with 5% BSA in PBS over night at 4 °C and treated with Hsp90 antibody (1:1000 dilution) for 3 h, and then with Rhodamine-conjugated goat anti-rabbit IgG (1:500, Millipore) for 1 h at RT. Nuclei were stained by using DAPI.

To observe the cellular localization of viral and host proteins in absence or presence of GA, Sf9 cells (2×10^6) were infected with vAc-*egfp* at an MOI of 5 or transfected with plasmid pIZ/V5-*actin-egfp* or pIZ/V5-*p40*-HA followed by super-infection with vAc-*rfp*. After 1 h of incubation, the supernatant was removed, and cells were treated with GA (1.25 μM) or DMSO. At different times p.i., the cells were fixed with 4% paraformaldehyde and then permeabilized with 0.2% Triton X-100. The cells were blocked with 5% BSA in PBS overnight at 4 °C and treated with the corresponding polyclonal antibodies (1:1000 dilution) or with anti-HA monoclonal antibody (1: 1000 dilution) for 3 h, and

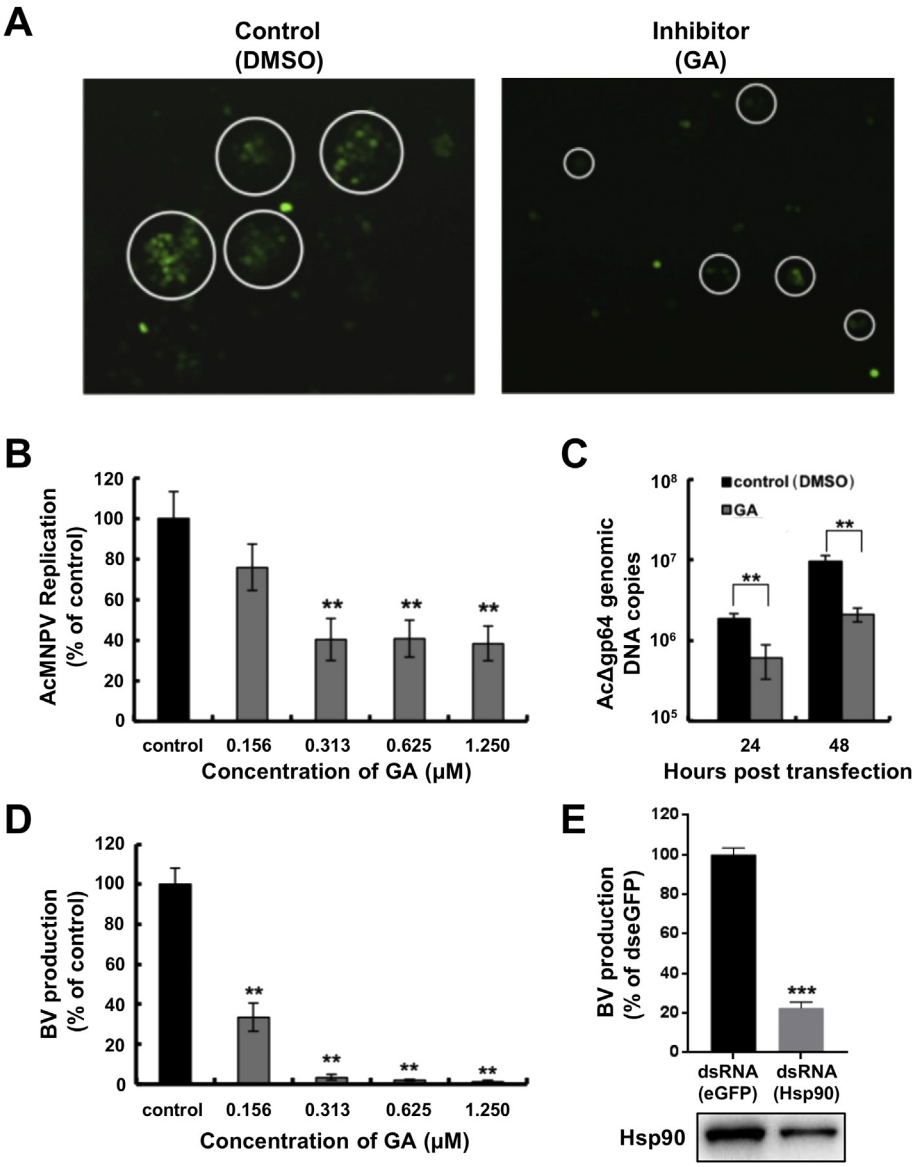

Fig. 2. Analysis of viral replication and BV production in the presence of GA or hsp90-specific dsRNA. (A) Plaque formation in AcMNPV infected cells. Sf9 cells were infected with vAc-*egfp* at an MOI of 0.01 and treated with GA (1.25 μM) or DMSO control. Plaque formation was observed under a fluorescent microscope at 48 h p.i.. Analysis of AcMNPV replication (B) and BV production (D) in the presence of GA. vAc-*egfp* infected cells were treated with increasing concentrations of GA. At 24 h p.i., viral genomic DNA copies in infected cells or in supernatants was quantified by qPCR. (C) Quantitative analysis of viral DNA replication under GA treatment. Sf9 cells were transfected with Ac△*gp64* bacmid, followed by GA (1.25 μM) treatment. At 24 h and 48 h p.t., viral DNA in transfected cells was quantified by qPCR. (E) Analysis of BV production upon RNAi of Hsp90. Sf9 were transfected with hsp90-specific dsRNA or non-specific dsRNA targeting eGFP, followed by infection with AcMNPV at 24 h p.t.. BV production in the supernatant was detected by qPCR at 24 h p.i.. For B-E, the data are from three independent experiments. Error bars represent standard deviation. Data were analyzed by a two-tails student *t*-test, ** represents $P < 0.01$, *** represents $P < 0.001$.

then with Rhodamine-conjugated goat anti-rabbit IgG (1:500, Millipore) or FITC-conjugated goat anti-mouse IgG (1:500, Proteintech) for 1 h at RT. For staining of F-actin, Rhodamine-labeled phalloidin (Invitrogen) was incubated with cells for 45 min at RT. Nuclei were stained by using DAPI. The subcellular localization of proteins was detected by fluorescence microscopy.

2.10. Statistical analyses

A two-tailed Student's *t*-test was used to assume unequal variances for statistical comparisons, and a P value of < 0.05 was considered to be statistically significant.

3. Results

3.1. Localization of Hsp90 in AcMNPV virions and in infected insect cells

Previous studies suggested that host chaperone Hsp90 was incorporated into baculovirus virions and might be involved in the life cycle of baculovirus (Hou et al., 2013; Lyupina et al., 2011). We firstly investigated the localization of Hsp90 in AcMNPV particles. BV or ODV particles were purified and separated into their nucleocapsid- and envelope fractions by ultracentrifugation and the samples were analyzed by Western blots. As shown in Fig. 1A (upper panel), Hsp90 is in the nucleocapsid fractions (lane NC), but not in the envelope fractions (lane E) of BVs. No Hsp90 was detected in the nucleocapsid or envelope fractions of ODVs. The specificity of *anti*-Hsp90 antibody was confirmed by RNAi and over-expression experiments (data not shown). The ODV envelop protein ODV-E66, BV envelope protein GP64 and the major nucleocapsid protein VP39 served as controls (Fig. 1A, lower panels). These results demonstrated that Hsp90 is associated exclusively with the nucleocapsid fractions of AcMNPV BV.

To investigate the subcellular localization of Hsp90, IF microscopy was conducted by using an antibody against Hsp90. As shown in Fig. 1B, Hsp90 was mainly localized in the cytoplasm in mock-infected cells. Upon AcMNPV infection, Hsp90 was translocated into the nucleus since 24 h p.i., and the fluorescence was seen in the whole cell at later time points (Fig. 1B). This result was further supported by expression of Hsp90 fused with eGFP protein. Sf9 cells were transfected with the plasmid expressing fusion proteins, followed by super-infection with AcMNPV, the fluorescence signal of eGFP could be observed in nucleus of infected cell (Fig. S1). Analysis of Hsp90 expression levels during infection revealed no obvious changes (Fig. 1C), confirming the results of Lyupina et al. (2011).

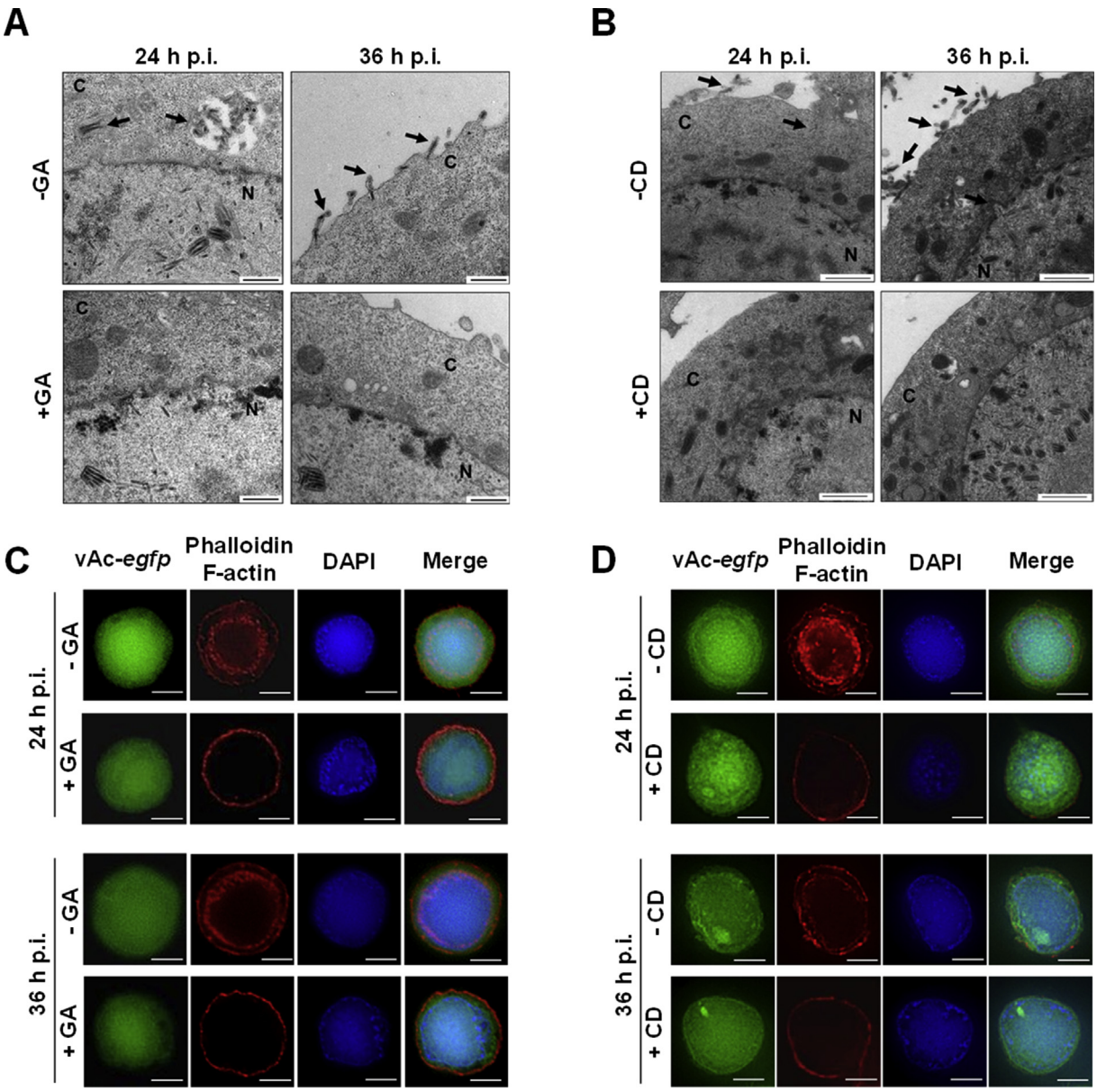

Fig. 3. Influence of GA and CD on AcMNPV budding and virus-induced nuclear F-actin polymerization. (A) EM observation of AcMNPV budding following GA treatment. Sf9 cells were infected with vAc-*egfp* (MOI = 5) and treated with GA (1.25 μM) or control DMSO. Trafficking of nucleocapsids (indicated by arrows) within infected cells was observed by EM. C: Cytoplasm, N: Nucleus. (B) EM observation of AcMNPV budding following CD treatment. Sf9 cells were infected with vAc-*egfp*, followed by treatment with CD (2 μg/ml) or control DMSO. At 24 and 36 h p.i, nucleocapsids trafficking within infected cells was observed by EM (indicated by arrows). C: Cytoplasm, N: Nucleus. Bars, 1 μm. (C) Inhibition of actin polymerization in infected cells by GA treatment. Sf9 cells were infected with vAc-*egfp* (MOI = 5). At 24 or 36 h p.i., F-actin was stained with Rhodamine-labeled phalloidin and nuclei were stained with DAPI. Signals were detected by fluorescence microscopy. Bars represent 5 μm. (D) Inhibition of actin polymerization in infected cells by CD treatment. Sf9 cells were infected with vAc-*egfp* (MOI = 5) and treated with CD (2 μg/ml) or control DMSO. At 24 or 36 h p.i., F-actin was stained with Rhodamine-labeled phalloidin and nuclei were stained with DAPI. Bars represent 5 μm.

3.2. Hsp90 is indispensable for infectious BV production

Infection studies were performed, and GA (a specific inhibitor of Hsp90) was used to determine the effects of Hsp90 on virus replication. After confirming that GA had no cytotoxic effect below 2.5 μM on Sf9 cells by the Trypan blue staining assay (data not show), we conducted a plaque assay to compare foci size in Sf9 cells infected with vAc-*egfp* followed by treatment of GA (1.25 μM) or control (DMSO). At 48 h p.i., the sizes of plaques were significantly smaller in the GA-treated group compared to that of the control group (Fig. 2A). These results suggested that Hsp90 might be involved in the spread of the BV phenotypes of AcMNPV.

To examine the role of Hsp90 in AcMNPV DNA replication, Real-Time qPCR assays were performed on samples of cells and supernatant fluids taken periodically in time course studies. The results showed that GA had an obvious inhibitory effect on the viral DNA replication. At drug concentrations above 0.313 μM, viral DNA accumulation reduced by ~60% ($P < 0.01$) (Fig. 2B). Viral DNA replication was further analyzed by using a *gp64*-knock out bacmid (AcΔ*gp64*), which is unable to produce infectious BV for secondary infection, but is not compromised in viral DNA replication. The result showed that in the presence of Hsp90 inhibitor, the DNA replication of AcΔ*gp64* decreased 3–4 fold at 24 and 48 h p.t. ($P < 0.01$) (Fig. 2C). In addition, GA suppressed BV production in a dose dependent manner and BV production decreased

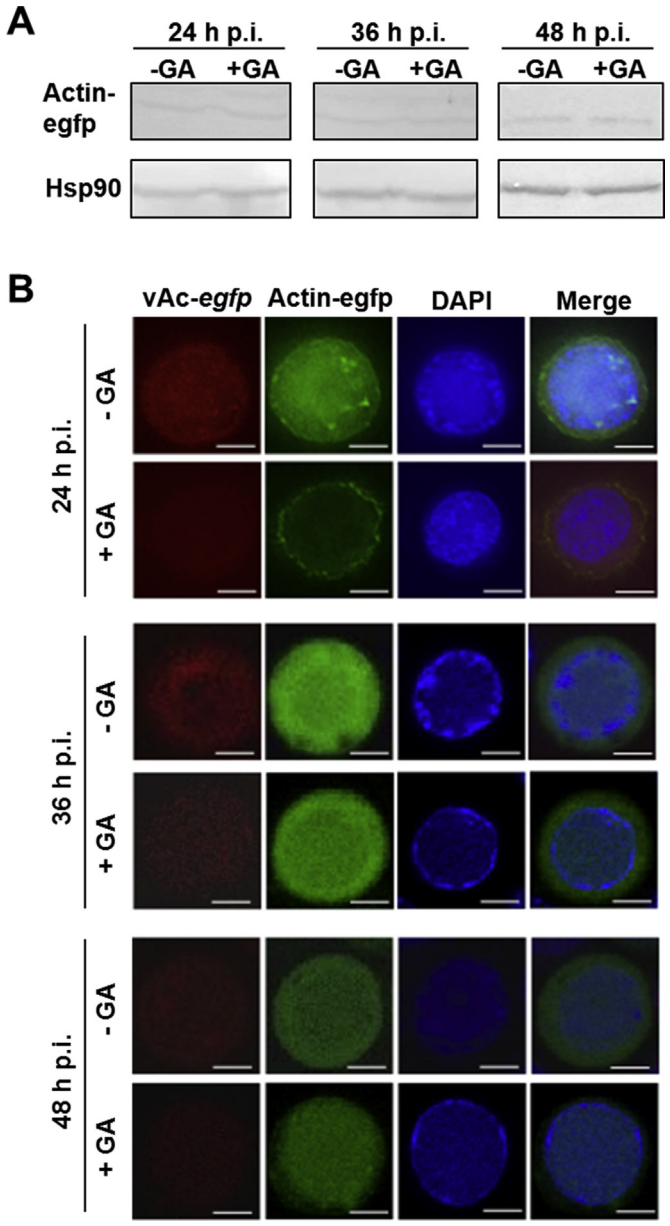

Fig. 4. Influence of GA on protein abundance and nuclear translocation of G-actin. (A) The influence of GA on protein abundance of G-actin. Sf9 cells were transfected with pIZ/V5-*actin-egfp*. At 24 h p.t., cells were super-infected with vAc-*rfp*, followed by addition of GA or control DMSO. Infected cells were analyzed by Western blot using *anti*-EGFP antibody. (B) Subcellular localization of actin in the presence of GA. Sf9 cells were transfected with pIZ/V5-*actin-egfp*. At 24 h p.t., cells were infected with vAc-*rfp*, followed by addition of GA or control DMSO. The localization of actin in infected cells was analyzed by IF microscopy using *anti*-EGFP antibody.

by ~98% at a concentration of 1.25 μM (Fig. 2D). To confirm the results of the GA experiments were not due to off-target effects, we conducted RNAi experiments wherein cells were treated with Hsp90-specific dsRNA then infected with AcMNPV. In dsRNA treated cells, the abundance of Hsp90 reduced to ~35% and the BV production decreased to ~25% ($P < 0.001$) (Fig. 2E). Together with the GA experimental results, these results suggested that Hsp90 played an important role in DNA replication and an even more significant role in BV production.

3.3. Hsp90 assists in morphogenesis of AcMNPV BV phenotype

To test whether Hsp90 is involved in the BV formation and budding, we examined the intracellular trafficking of nucleocapsids and budding of BVs by EM. At 24 and 36 h p.i., the assembled nucleocapsids could be observed under GA treatment (Fig. 3A). The number of nucleocapsids in the nuclei decreased to ~50% of the control group in the presence of GA at 24 h p.i., and then fully recovered at 36 h p.i. (data not shown), suggesting that GA delayed the assembly of progeny nucleocapsids. In the absence of GA, the egress of nucleocapsids from the nucleus and the trafficking to the cytoplasm was easily captured at 24 h p.i., and budding through plasma membrane frequently occurred at 36 h p.i. (Fig. 3A, upper panel, indicated by arrowheads). In contrast, when GA was added, only very few nucleocapsids entered the cytoplasm at 24 h p.i.; budding of nucleocapsids was barely detected at 36 h p.i. (Fig. 3A, lower panel). The number of virus in budding process under GA treatment was also counted. The result indicated that virus budding decreased severely (> 80%) in GA treated group compared to the control group (data not shown). This was further confirmed by RNAi experiment that in hsp90-specific dsRNA treated group, the overall number of virus budding is much less than that of the control group (dseGFP) group (data not shown).

3.4. Inhibition of Hsp90 significantly suppresses host nuclear actin polymerization which is required for BV production

The nuclear (F-actin) has long been known to be required for AcMNPV infection and morphogenesis (Lanier and Volkman, 1998; Ohkawa and Volkman, 1999). A recent study identified a crucial role of nuclear F-actin in the egress of progeny viral nucleocapsids from the nucleus to the cytoplasm for BV formation (Ohkawa and Welch, 2018). When actin polymerization was abolished by a specific inhibitor CD, the plaque size decreased significantly (data not shown). In addition, nucleocapsids failed to egress from nucleus and BV budding was completely blocked (Fig. 3B), a similar trend to that of GA treatment, albeit CD showed a higher inhibitory effect than GA (Fig. 3A). Hsp90 is able to interact with and stimulate the phosphorylation of Neural Wiskott-Aldrich syndrome protein (N-WASP) in mammalian cells, which resulted in an N-WASP-induced actin polymerization (Park et al., 2005). We, therefore, asked whether Hsp90 was involved in polymerization of actin during AcMNPV infection. In the absence of GA, F-actin was observed both around the cell periphery and nuclear envelope. In the presence of GA, the signal of nuclear F-actin was almost undectable (Fig. 3C), which was had a similar trend with that of CD treatment (Fig. 3D).

3.5. Inactivation of Hsp90 has only minor impact on G-actin abundance and nuclear localization

Since nuclear transportation of globular actin (G-actin) is a prerequisite for actin polymerization within the nucleus, we questioned whether the inactivation of Hsp90 resulted in inadequate protein levels or nuclear accumulation of G-actin and subsequent prevented actin polymerization. In the presence of GA, the amounts of actin remained largely unchanged, suggesting that Hsp90 was not involved in the protein abundance of actin (Fig. 4A). When Sf9 cells were transfected with pIZ/V5-*actin-egfp,* fluorescence was diffused throughout the cytoplasm (data not shown). After transfected cells were subsequently infected with vAc-*rfp*, actin was detected in both the cytoplasm and nucleus at 24 h p.i. (Fig. 4B), which is consistent with previous observations (Gandhi et al., 2012; Ohkawa et al., 2002). In the presence of GA, however, the majority of actin was still cytoplasmic by 24 h p.i. (Fig. 4B), but by 36 and 48 h p.i., was clearly present in the nucleus as well (Fig. 4B). Inhibition of Hsp90, therefore, delayed but did not completely block the nuclear localization of G-actin during AcMNPV infection.

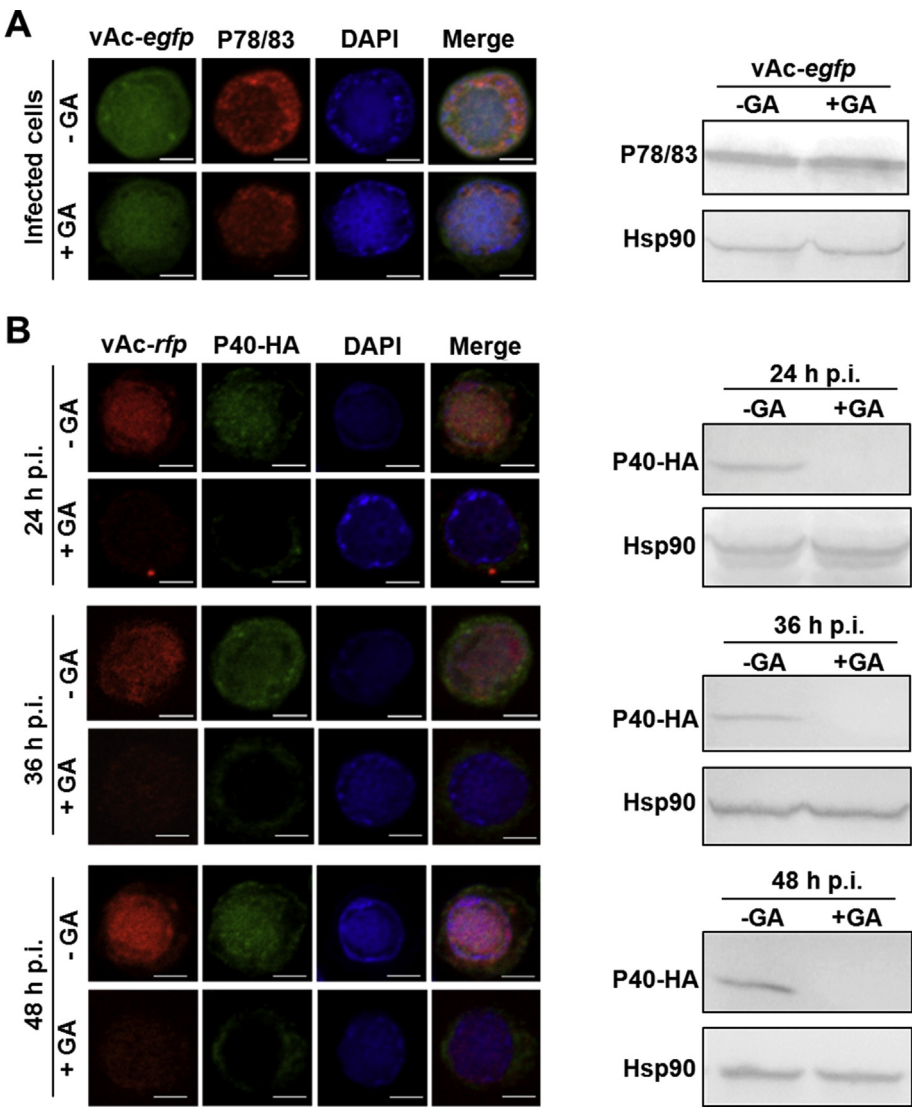

Fig. 5. The influence of GA on abundance and nuclear translocation of viral N-WASP like protein P78/83 and host Arp2/3 complex protein P40. For the detection of P78/83 abundance and translocation, Sf9 cells were infected with vAc-*egfp*, following by incubation with GA or DMSO control. At 48 h p.i., the abundance and subcellular distribution of P78/83 in infected cells was analyzed by Western blots and IF microscopy. For the detection of P40 expression and localization, Sf9 cells were transfected with pIZ/V5-*p40*-HA, followed by infection with vAc-*rfp* (MOI = 5) at 24 h p.t., treated with either GA or DMSO and collected at 24, 36 and 48 h post drug treatment. All the samples were analyzed by Western blots and IF microscopy. Nuclei were stained with DAPI. Bars, 5 μm.

3.6. Hsp90 promotes the formation of nuclear F-actin via regulating the P40 subunit of Arp2/3 complex

During late gene expression after successful nuclear translocation of actin, G-actin polymerizes within the nucleus of baculovirus infected cells. This process is dependent upon the nuclear localization and function of the host Arp2/3 complex and the viral N-WASP like protein P78/83 (Goley et al., 2006). We found that neither the protein levels nor the nuclear import of the viral P78/83 was affected by the presence of GA (Fig. 5A); implying P78/83 was not responsible for lack of nuclear actin polymerization. The Arp2/3 complex was next most likely possibility for the defect.

We investigated whether the protein abundance or localization of main components of Arp2/3 complex were affected, when the function of Hsp90 was disturbed. Arp2/3 complex contains seven subunits, Arp2, Arp3, P40/ARPC1 (P40), P34/ARPC2 (P34), P21/ARPC3 (P21), P20/ARPC4 (P20) and P16/ARPC5 (P16) (Goley and Welch, 2006; Mu et al., 2016). Among these, P40 interacts with N-WASP like protein P78/83 (Han et al., 2012). We, therefore, determined whether Sf-P40 was the main target in the regulation of nuclear actin polymerization. The expression and subcellular localization of P40 were detected by Western blot and IF microscopy, respectively. In the presence of GA, the expression of P40, decreased to undetectable level (Fig. 5B). Furthermore, no obvious P40 fluorescence signal was detected in nucleus under the treatment of GA, suggesting that the translocation of P40 into nucleus mediated by AcMNPV infection was hindered, due to the inactivation of Hsp90 (Fig. 5B).

For the rest six subunits, the IF microscopy revealed that all the six components showed similar subcellular localization pattern in the presence or absence of GA, distributing evenly in both cytoplasm and nucleus upon AcMNPV infection (Fig. S2). In addition, no obvious differences in protein abundance were observed under IF detection. Therefore, in contrast to the mechanism in mammalian cells, Hsp90 is involved in AcMNPV-triggered nuclear actin polymerization in insect cells through regulation of host Arp2/3 complex, exclusively P40, but not the N-WASP like protein.

4. Discussion

In this study, Hsp90 was identified as an essential host factor for baculovirus BV morphogenesis. When the activity of Hsp90 was inhibited, newly assembled nucelocapsids gathered around inner nuclear membrane could be detected and only very few entered the cytoplasm and release of BV particles was reduced severely (Figs. 2D and 3A). GA treatment resulted in reduction in viral DNA replication (Fig. 2B and C), which is in agreement with a previous report (Lyupina et al., 2011). Hsp90 was reported to facilitate virus replication by promoting polymerase stabilization (Katoh et al., 2017), which might provide an

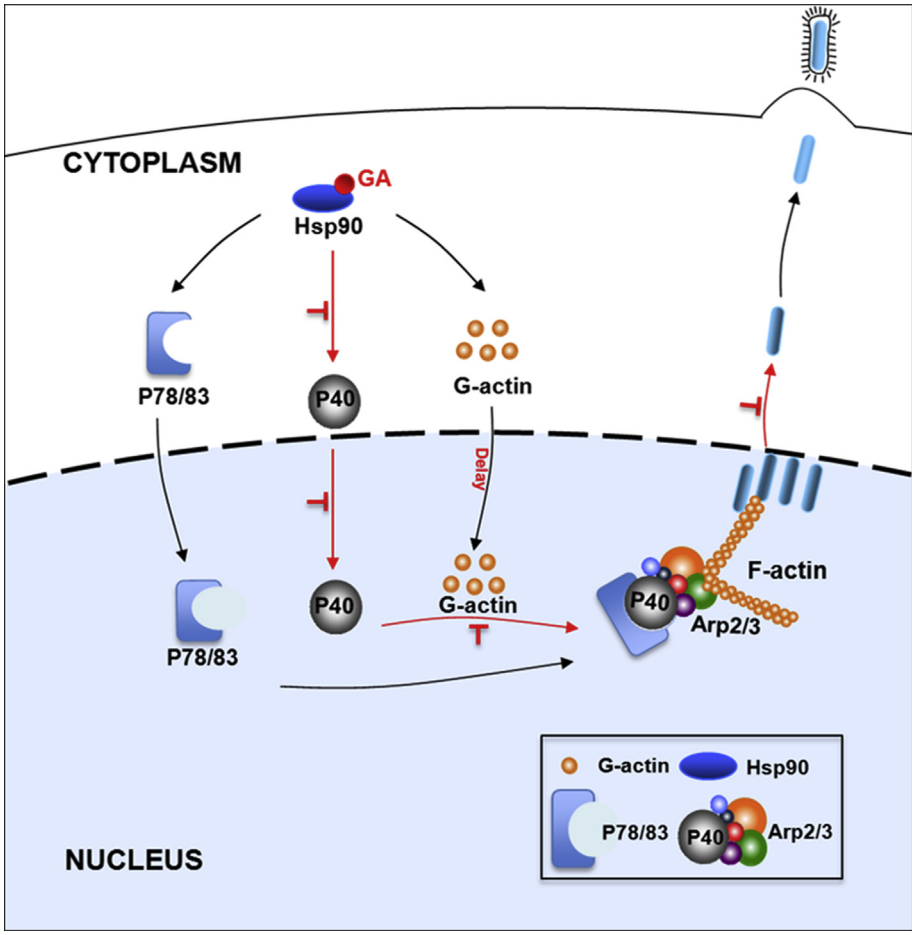

Fig. 6. Proposed functional model of Hsp90 in baculovirus BV formation. Based on our results, hsp90 are identified as an essential host factor for BV formation. When the function of Hsp90 was inhibited, virus-triggered host nuclear actin polymerization was significantly blocked probably due to inadequate protein amounts and mis-localization of Arp2/3-P40, and this leads to block of BV egress and production.

explanation to the function of Hsp90 in AcMNPV DNA replication.

Production of BV requires proper assembly of progeny nucleocapsids and their transfer to cytoplasm for subsequent virus budding. When the function of Hsp90 was inhibited, assembled nucleocapsids could be detected either around the ring zone or the nuclear periphery, with only very few nucleocapsids egressing from the nucleus to the cytoplasm for BV budding (Fig. 3A). Hsp90 was identified as an actin-binding protein, facilitating the actin polymerization to promote the formation of filopodia (Taiyab and Rao Ch, 2011), and a recent study indicated that nuclear actin is crucial for viral egress from the nucleus (Ohkawa and Welch, 2018). Thus, we further detected the formation of virus-induced nuclear F-actin (Fig. 3C) and the results indicated that the lack of nuclear F-actin scaffold for nucleocapsid exportation is one logical explanation for much reduced BV production when Hsp90 was inhibited (Fig. 2D and E and 3A). On the other hand, Hsp90 inhibitor was reported to inhibit human DNA topoisomerase II, and the latter was proposed to play a role in baculovirus DNA processing under the regulation of F-actin (Volkman, 2015). Therefore, Hsp90 and F-actin may also be involved in genome processing of baculovirus to some extent, although nucleocapsids with normal morphology are detected in the presence of GA.

In mammalian cells, Hsp90 is involved in N-WASP-mediated actin polymerization. Binding of Hsp90 to N-WASP protein increases the activation of N-WASP protein, and protects of activated N-WASP protein from proteasome-dependent degradation (Park et al., 2005). In insect cells infected with baculovirus, virus-induced nuclear accumulation and polymerization of actin are mediated by multiple viral proteins acting in concert with host factors (Lanier and Volkman, 1998; Ohkawa and Volkman, 1999; Park et al., 2005). The recruitment of G-actin into nucleus was found to be delayed by the Hsp90 inhibitor (Fig. 4B), an effect similar to the lack of *pe38* expression, one of the six AcMNPV early genes that mediate nuclear localization of G-actin (Gandhi et al., 2012; Ohkawa et al., 2002). The viral N-WASP like protein P78/83 and host Arp2/3 complex play crucial roles in actin polymerization within the infected nucleus (Charlton and Volkman, 1991; Hess et al., 1989; Volkman et al., 1987). We showed that inhibition of Hsp90 had no effect on the protein levels and nuclear import of P78/83 (Fig. 5A); instead, the protein level and nuclear import of P40, a subunit of Arp2/3 complex which interacts with P78/83 (Han et al., 2012), was reduced dramatically (Fig. 5B). However, the protein levels and nuclear relocation of the rest six components of Arp2/3 complex, including Arp2, Arp3, P34, P21, P20 and P16 upon AcMNPV infection was not affected when the function of Hsp90 was disturbed (Fig. S2). Further investigation indicated that the decreased abundance of P40 under GA treatment could not be rescued by the proteasome inhibitor MG132, lysosome inhibitor chloroquine or autophagy inhibitor 3 MA (data not shown). In addition, no direct interaction between Hsp90 and P40 was detected by immunoprecipitation, suggesting that Hsp90 regulates the accumulation of P40 indirectly through an unknown mechanism. We proposed that Hsp90 selectively targeted the P40 subunit of Arp2/3 complex to regulate actin nuclear polymerization. So far, it is still unclear whether such a big Arp2/3 complex enters nucleus entirely or the seven subunits enter nucleus individually before they assemble into a complex. Based on the fact that the nuclear relocation of other components of Arp2/3 complex was not affected by the retention of P40, we speculate that the Arp2/3 complex may translocate to the nucleus individually. This speculation is consistent with a previous report, which also proposed that Arp2/3 may recruited to the nucleus as an individual subunit (Mu et al., 2016).

In summary, we identified that molecular chaperon Hsp90 plays a

crucial role in AcMNPV infection process, particularly in the steps of BV morphogenesis. Subsequently, we explored how Hsp90 regulates AcMNPV infection. As proposed in Fig. 6, Hsp90 facilitates the protein accumulation and nuclear transportation of Arp2/3-P40, an actin-nucleating factor required for virus-triggered formation of nuclear F-actin. The polymerized nuclear F-actin further provides essential driving forces for the egress of nucleocapsids from the infected nucleus for further BV formation. Thus we offer an interpretation of the cause-and-effect relationship between Hsp90 and P40 with the phenomena of defective BV production and maturation based on our findings. Further investigations into this point will shed light on the biological functions of Hsp90, as well as the mechanism of baculovirus-induced host cell actin polymerization.

Acknowledgments

This work was supported by grants from the National Natural Science Foundation of China (31572334 and 31621061), the Strategic Priority Research Program of the Chinese Academy of Sciences (XDB11030400). We thank Dr. Basil M. Arif and Dr. Loy Volkman for scientific editing of the manuscript. We thank Ms Youling Zhu, Mr Fan Zhang and Ms Xuefang An from the Experimental Animal center, Wuhan Institute of Virology for help in antibody preparation. We acknowledge Dr Ding Gao, Ms Anna Du, Ms Bichao Xu, Ms Pei Zhang and Ms Juan Min from the Center for Instrumental Analysis and Metrology, Wuhan Institute of Virology, Chinese Academy of Science for technical assistance.

Appendix A. Supplementary data

Supplementary data to this article can be found online at https://doi.org/10.1016/j.virol.2019.07.006.

References

Burch, A.D., Weller, S.K., 2005. Herpes simplex virus type 1 DNA polymerase requires the mammalian chaperone hsp90 for proper localization to the nucleus. J. Virol. 79, 10740–10749.
Charlton, C.A., Volkman, L.E., 1991. Sequential rearrangement and nuclear polymerization of actin in baculovirus-infected Spodoptera frugiperda cells. J. Virol. 65, 1219–1227.
Charlton, C.A., Volkman, L.E., 1993. Penetration of Autographa californica nuclear polyhedrosis virus nucleocapsids into IPLB Sf 21 cells induces actin cable formation. Virology 197, 245–254.
Chen, Y.R., Zhong, S., Fei, Z., Hashimoto, Y., Xiang, J.Z., Zhang, S., Blissard, G.W., 2013. The transcriptome of the baculovirus Autographa californica multiple nucleopolyhedrovirus in Trichoplusia ni cells. J. Virol. 87, 6391–6405.
Das, I., Basantray, I., Mamidi, P., Nayak, T.K., B, M.P., Chattopadhyay, S., Chattopadhyay, S., 2014. Heat shock protein 90 positively regulates Chikungunya virus replication by stabilizing viral non-structural protein nsP2 during infection. PLoS One 9, e100531.
de Chassey, B., Navratil, V., Tafforeau, L., Hiet, M.S., Aublin-Gex, A., Agaugue, S., Meiffren, G., Pradezynski, F., Faria, B.F., Chantier, T., Le Breton, M., Pellet, J., Davoust, N., Mangeot, P.E., Chaboud, A., Penin, F., Jacob, Y., Vidalain, P.O., Vidal, M., Andre, P., Rabourdin-Combe, C., Lotteau, V., 2008. Hepatitis C virus infection protein network. Mol. Syst. Biol. 4, 230.
Dong, S., Wang, M., Qiu, Z., Deng, F., Vlak, J.M., Hu, Z., Wang, H., 2010. Autographa californica multicapsid nucleopolyhedrovirus efficiently infects Sf9 cells and transduces mammalian cells via direct fusion with the plasma membrane at low pH. J. Virol. 84, 5351–5359.
Gandhi, K.M., Ohkawa, T., Welch, M.D., Volkman, L.E., 2012. Nuclear localization of actin requires AC102 in Autographa californica multiple nucleopolyhedrovirus-infected cells. J. Gen. Virol. 93, 1795–1803.
Ghosh, S., Parvez, M.K., Banerjee, K., Sarin, S.K., Hasnain, S.E., 2002. Baculovirus as mammalian cell expression vector for gene therapy: an emerging strategy. Mol. Ther. 6, 5–11.
Goley, E.D., Ohkawa, T., Mancuso, J., Woodruff, J.B., D'Alessio, J.A., Cande, W.Z., Volkman, L.E., Welch, M.D., 2006. Dynamic nuclear actin assembly by Arp2/3 complex and a baculovirus WASP-like protein. Science 314, 464–467.
Goley, E.D., Welch, M.D., 2006. The ARP2/3 complex: an actin nucleator comes of age. Nat. Rev. Mol. Cell Biol. 7, 713–726.
Han, S.L., Mu, J.F., Zhang, Y.L., Chen, X.W., Wang, Y., Li, L.L., 2012. Cloning and functional research of Arp2/3-P40/ARPC1 subunit of Sf9 cells. Bingdu Xuebao 28, 601–608.
Hess, R.T., Goldsmith, P.A., Volkman, L.E., 1989. Effect of cytochalasin D on cell morphology and AcMNPV replication in a Spodoptera frugiperda cell line. J. Invertebr. Pathol. 53, 169–182.
Hou, D., Zhang, L., Deng, F., Fang, W., Wang, R., Liu, X., Guo, L., Rayner, S., Chen, X., Wang, H., Hu, Z., 2013. Comparative proteomics reveal fundamental structural and functional differences between the two progeny phenotypes of a baculovirus. J. Virol. 87, 829–839.
Hu, J., Seeger, C., 1996. Hsp90 is required for the activity of a hepatitis B virus reverse transcriptase. Proc. Natl. Acad. Sci. U. S. A. 93, 1060–1064.
Inceoglu, A.B., Kamita, S.G., Hinton, A.C., Huang, Q., Severson, T.F., Kang, K., Hammock, B.D., 2001. Recombinant baculoviruses for insect control. Pest Manag. Sci. 57, 981–987.
Jackson, S.E., 2013. Hsp90: structure and function. Top. Curr. Chem. 328, 155–240.
Jager, S., Cimermancic, P., Gulbahce, N., Johnson, J.R., McGovern, K.E., Clarke, S.C., Shales, M., Mercenne, G., Pache, L., Li, K., Hernandez, H., Jang, G.M., Roth, S.L., Akiva, E., Marlett, J., Stephens, M., D'Orso, I., Fernandes, J., Fahey, M., Mahon, C., O'Donoghue, A.J., Todorovic, A., Morris, J.H., Maltby, D.A., Alber, T., Cagney, G., Bushman, F.D., Young, J.A., Chanda, S.K., Sundquist, W.I., Kortemme, T., Hernandez, R.D., Craik, C.S., Burlingame, A., Sali, A., Frankel, A.D., Krogan, N.J., 2012. Global landscape of HIV-human protein complexes. Nature 481, 365–370.
Kasman, L.M., Volkman, L.E., 2000. Filamentous actin is required for lepidopteran nucleopolyhedrovirus progeny production. J. Gen. Virol. 81, 1881–1888.
Katoh, H., Kubota, T., Nakatsu, Y., Tahara, M., Kidokoro, M., Takeda, M., 2017. Heat shock protein 90 ensures efficient mumps virus replication by assisting with viral polymerase complex formation. J. Virol. 91.
Keddie, B.A., Aponte, G.W., Volkman, L.E., 1989. The pathway of infection of Autographa californica nuclear polyhedrosis virus in an insect host. Science 243, 1728–1730.
Kidd, I.M., Emery, V.C., 1993. The use of baculoviruses as expression vectors. Appl. Biochem. Biotechnol. 42, 137–159.
Landais, I., Pommet, J., Mita, K., Nohata, J., Gimenez, S., Fournier, P., Devauchelle, G., Duonor-Cerutti, M., Ogliastro, M., 2001. Characterization of the cDNA encoding the 90 kDa heat-shock protein in the Lepidoptera Bombyx mori and Spodoptera frugiperda. Gene 271, 223–231.
Lanier, L.M., Volkman, L.E., 1998. Actin binding and nucleation by Autographa california M nucleopolyhedrovirus. Virology 243, 167–177.
Li, Y., Shen, S., Hu, L., Deng, F., Vlak, J.M., Hu, Z., Wang, H., Wang, M., 2018. The functional oligomeric state of tegument protein GP41 is essential for baculovirus budded virion and occlusion-derived virion assembly. J. Virol. 92.
Li, Y., Zhang, T., Schwartz, S.J., Sun, D., 2009. New developments in Hsp90 inhibitors as anti-cancer therapeutics: mechanisms, clinical perspective and more potential. Drug Resist. Updates 12, 17–27.
Lin, T.W., Lo, C.W., Lai, S.Y., Fan, R.J., Lo, C.J., Chou, Y.M., Thiruvengadam, R., Wang, A.H., Wang, M.Y., 2007. Chicken heat shock protein 90 is a component of the putative cellular receptor complex of infectious bursal disease virus. J. Virol. 81, 8730–8741.
Lyupina, Y.V., Zatsepina, O.G., Timokhova, A.V., Orlova, O.V., Kostyuchenko, M.V., Beljelarskaya, S.N., Evgen'ev, M.B., Mikhailov, V.S., 2011. New insights into the induction of the heat shock proteins in baculovirus infected insect cells. Virology 421, 34–41.
McClellan, A.J., Frydman, J., 2001. Molecular chaperones and the art of recognizing a lost cause. Nat. Cell Biol. 3, E51–E53.
Miyata, Y., Yahara, I., 2000. p53-independent association between SV40 large T antigen and the major cytosolic heat shock protein, HSP90. Oncogene 19, 1477–1484.
Mu, J., Zhang, Y., Hu, Y., Hu, X., Zhou, Y., Chen, X., Wang, Y., 2016. The role of viral protein Ac34 in nuclear relocation of subunits of the actin-related protein 2/3 complex. Virol. Sin. 31, 480–489.
Naito, T., Momose, F., Kawaguchi, A., Nagata, K., 2007. Involvement of Hsp90 in assembly and nuclear import of influenza virus RNA polymerase subunits. J. Virol. 81, 1339–1349.
Ohkawa, T., Rowe, A.R., Volkman, L.E., 2002. Identification of six Autographa californica multicapsid nucleopolyhedrovirus early genes that mediate nuclear localization of G-actin. J. Virol. 76, 12281–12289.
Ohkawa, T., Volkman, L.E., 1999. Nuclear F-actin is required for AcMNPV nucleocapsid morphogenesis. Virology 264, 1–4.
Ohkawa, T., Welch, M.D., 2018. Baculovirus actin-based motility drives nuclear envelope disruption and nuclear egress. Curr. Biol. 28, 2153–2159 e2154.
Park, S.J., Suetsugu, S., Takenawa, T., 2005. Interaction of HSP90 to N-WASP leads to activation and protection from proteasome-dependent degradation. EMBO J. 24, 1557–1570.
Pearl, L.H., Prodromou, C., 2006. Structure and mechanism of the Hsp90 molecular chaperone machinery. Annu. Rev. Biochem. 75, 271–294.
Picard, D., 2002. Heat-shock protein 90, a chaperone for folding and regulation. Cell. Mol. Life Sci. 59, 1640–1648.
Pratt, W.B., Toft, D.O., 2003. Regulation of signaling protein function and trafficking by the hsp90/hsp70-based chaperone machinery. Exp. Biol. Med. 228, 111–133.
Radhakrishnan, A., Yeo, D., Brown, G., Myaing, M.Z., Iyer, L.R., Fleck, R., Tan, B.H., Aitken, J., Sanmun, D., Tang, K., Yarwood, A., Brink, J., Sugrue, R.J., 2010. Protein analysis of purified respiratory syncytial virus particles reveals an important role for heat shock protein 90 in virus particle assembly. Mol. Cell. Proteom. 9, 1829–1848.
Reyes-Del Valle, J., Chavez-Salinas, S., Medina, F., Del Angel, R.M., 2005. Heat shock protein 90 and heat shock protein 70 are components of dengue virus receptor complex in human cells. J. Virol. 79, 4557–4567.
Smith, D.R., McCarthy, S., Chrovian, A., Olinger, G., Stossel, A., Geisbert, T.W., Hensley, L.E., Connor, J.H., 2010. Inhibition of heat-shock protein 90 reduces Ebola virus replication. Antivir. Res. 87, 187–194.
Summers, M.D., 1971. Electron microscopic observations on granulosis virus entry, uncoating and replication processes during infection of the midgut cells of Trichoplusia ni. J. Ultrastruct. Res. 35, 606–625.

Taiyab, A., Rao Ch, M., 2011. HSP90 modulates actin dynamics: inhibition of HSP90 leads to decreased cell motility and impairs invasion. Biochim. Biophys. Acta 1813, 213–221.

Tsou, Y.L., Lin, Y.W., Chang, H.W., Lin, H.Y., Shao, H.Y., Yu, S.L., Liu, C.C., Chitra, E., Sia, C., Chow, Y.H., 2013. Heat shock protein 90: role in enterovirus 71 entry and assembly and potential target for therapy. PLoS One 8, e77133.

Uetz, P., Dong, Y.A., Zeretzke, C., Atzler, C., Baiker, A., Berger, B., Rajagopala, S.V., Roupelieva, M., Rose, D., Fossum, E., Haas, J., 2006. Herpesviral protein networks and their interaction with the human proteome. Science 311, 239–242.

Ujino, S., Yamaguchi, S., Shimotohno, K., Takaku, H., 2009. Heat-shock protein 90 is essential for stabilization of the hepatitis C virus nonstructural protein NS3. J. Biol. Chem. 284, 6841–6846.

Vaughn, J.L., Goodwin, R.H., Tompkins, G.J., McCawley, P., 1977. The establishment of two cell lines from the insect Spodoptera frugiperda (Lepidoptera; Noctuidae). In Vitro 13, 213–217.

Volkman, L.E., 2015. Baculoviruses and nucleosome management. Virology 476, 257–263.

Volkman, L.E., Goldsmith, P.A., Hess, R.T., 1987. Evidence for microfilament involvement in budded Autographa californica nuclear polyhedrosis virus production. Virology 156, 32–39.

Volkman, L.E., Summers, M.D., 1977. Autographa californica nuclear polyhedrosis virus: comparative infectivity of the occluded, alkali-liberated, and nonoccluded forms. J. Invertebr. Pathol. 30, 102–103.

Wandinger, S.K., Richter, K., Buchner, J., 2008. The Hsp90 chaperone machinery. J. Biol. Chem. 283, 18473–18477.

Wang, M., Tan, Y., Yin, F., Deng, F., Vlak, J.M., Hu, Z., Wang, H., 2008a. The F-like protein Ac23 enhances the infectivity of the budded virus of gp64-null Autographa californica multinucleocapsid nucleopolyhedrovirus pseudotyped with baculovirus envelope fusion protein F. J. Virol. 82, 9800–9804.

Wang, M., Tuladhar, E., Shen, S., Wang, H., van Oers, M.M., Vlak, J.M., Westenberg, M., 2010a. Specificity of baculovirus P6.9 basic DNA-binding proteins and critical role of the C terminus in virion formation. J. Virol. 84, 8821–8828.

Wang, M., Yin, F., Shen, S., Tan, Y., Deng, F., Vlak, J.M., Hu, Z., Wang, H., 2010b. Partial functional rescue of Helicoverpa armigera single nucleocapsid nucleopolyhedrovirus infectivity by replacement of F protein with GP64 from Autographa californica multicapsid nucleopolyhedrovirus. J. Virol. 84, 11505–11514.

Wang, R., Deng, F., Hou, D., Zhao, Y., Guo, L., Wang, H., Hu, Z., 2010c. Proteomics of the Autographa californica nucleopolyhedrovirus budded virions. J. Virol. 84, 7233–7242.

Wang, X., Chen, C., Zhang, N., Li, J., Deng, F., Wang, H., Vlak, J.M., Hu, Z., Wang, M., 2018. The group I alphabaculovirus-specific protein, AC5, is a novel component of the occlusion body but is not associated with ODVs or the PIF complex. J. Gen. Virol. 99, 585–595.

Wang, Y., Wang, Q., Liang, C., Song, J., Li, N., Shi, H., Chen, X., 2008b. Autographa californica multiple nucleopolyhedrovirus nucleocapsid protein BV/ODV-C42 mediates the nuclear entry of P78/83. J. Virol. 82, 4554–4561.

Waxman, L., Whitney, M., Pollok, B.A., Kuo, L.C., Darke, P.L., 2001. Host cell factor requirement for hepatitis C virus enzyme maturation. Proc. Natl. Acad. Sci. U. S. A. 98, 13931–13935.

Zhang, Y., Hu, X., Mu, J., Hu, Y., Zhou, Y., Zhao, H., Wu, C., Pei, R., Chen, J., Chen, X., Wang, Y., 2018. Ac102 participates in nuclear actin polymerization by modulating BV/ODV-C42 ubiquitination during Autographa californica multiple nucleopolyhedrovirus infection. J. Virol. 92 pii: e00005-18.

Zheng, Z.Z., Miao, J., Zhao, M., Tang, M., Yeo, A.E., Yu, H., Zhang, J., Xia, N.S., 2010. Role of heat-shock protein 90 in hepatitis E virus capsid trafficking. J. Gen. Virol. 91, 1728–1736.

Zou, Z., Liu, J., Wang, Z., Deng, F., Wang, H., Hu, Z., Wang, M., Zhang, T., 2016. Characterization of two monoclonal antibodies, 38F10 and 44D11, against the major envelope fusion protein of Helicoverpa armigera nucleopolyhedrovirus. Virol. Sin. 31, 490–499.